

# Positive grid corrosion elongation analysis using CAE with corrosion deformation transformed into thermal phenomenon

Ichiroh Mukaitani<sup>a,b,\*</sup>, Koji Hayashi<sup>a</sup>, Ichiro Shimoura<sup>a</sup>, Arihiko Takemasa<sup>a</sup>,  
Isamu Takahashi<sup>c</sup>, Harushige Tsubakino<sup>d</sup>

<sup>a</sup> *Shin-Kobe Electric Machinery Co., Ltd., 1300-15 Yabata, Nabari, Mie 518-0625, Japan*

<sup>b</sup> *Graduate Student Hyogo University, 2167 Shosha, Himeji, Hyogo 671-2201, Japan*

<sup>c</sup> *Hitachi, Ltd., Hitachi Research Laboratory 1-1, Omika-cho 7-chome, Hitachi-shi Ibaraki-ken, 319-1292, Japan*

<sup>d</sup> *Department of Materials Science and Engineering, Hyogo University, 2167 Shosha, Himeji, Hyogo 671-2201, Japan*

## Abstract

Valve-regulated lead–acid (VRLA) batteries have been commercially available for more than 20 years and have been enthusiastically embraced by users of uninterruptible power supplies (UPS) because of the anticipated reduction in installation and operating costs, smaller footprint and fewer environmental concerns. In Japan, communication networks are demanding reduced costs and longer life from their batteries.

Among the factors limiting the life of VRLA batteries, the corrosion of positive grid material has been proven to cause elongation of the plates, loss of electrical contact and shorter lifetime. The content of Sn is also a key factor and addition of Sn in the grid alloy results in better performance in creep resistance, tensile strength and corrosion resistance [R. David Prenagaman, *The Battery Man*, vol. 39, September 1997, p. 16. I. Mukaitani, T. Sakamoto, T. Kikuoka, Y. Yamaguchi, H. Tsubakino, *Proceedings of the 40th Battery Symposium in Japan*, 1999, p. 99]. A key point is what the ratio of Sn to Ca should be, since too much Sn may lead to even worse elongation of the plates [I. Mukaitani, T. Sakamoto, T. Kikuoka, Y. Yamaguchi, H. Tsubakino, *Proceedings of the 40th Battery Symposium in Japan*, 1999, p. 99].

We have determined that microstructure control with a composition of lead–calcium–tin (Pb–Ca–Sn) alloy is optimal for better performance of the plates [I. Mukaitani, T. Sakamoto, T. Kikuoka, Y. Yamaguchi, H. Tsubakino, *Proceedings of the 40th Battery Symposium in Japan*, 1999, p. 99].

We developed a “simulation of current collector corrosion elongation” which is a technique of estimating corrosion elongation from the current collector design [I. Mukaitani, K. Hayashi, I. Shimoura, H. Takabayashi, M. Terada, A. Takemasa, I. Takahashi, K. Okamoto, *Proceedings of the 44th Battery Symposium in Japan*, 2003, p. 652]. Corrosion elongation occurs as the corrosion material layer grows out of the current collector metal. We resolved this problem using generally CAD software “*Solid Works*” and computer aided engineering (CAE) software “*ANSYS*” with corrosion elongation transformed into thermal elongation. We established a current collector corrosion elongation forecast and found that the microstructure controlled the Pb–Ca–Sn alloy; thus newly designed VRLA batteries (MU-series [A. Takemasa, I. Mukaitani, Y. Yoshiyama, K. Fukui, T. Sakamoto, T. Kuwano, M. Fukuda, H. Misaki, K. Uwatari, *Shin-Kobe Technical Report 9* (1999) 11] for telecommunication and LL-series [H. Takabayashi, T. Shibahara, Y. Mastuda, K. Fukui, S. Hazui, Y. Matsumura, S. Kondo, *Shin-Kobe Tech. Rep. 11* (2001) 35] for electric energy storage) which are lightweight and have long life are introduced here.

© 2004 Elsevier B.V. All rights reserved.

**Keywords:** VRLA batteries; Pb–Ca–Sn alloy; Computer aided engineering; Electric energy storage

## 1. Introduction

The communication network industry has been expanding in the Asia–Pacific area with the growth of mobile telecom-

munication service. Valve-regulated lead–acid (VRLA) batteries have been commercially available for more than 20 years and have been enthusiastically embraced by users of uninterruptible power supplies (UPS) because of the anticipated reduction in installation and operating costs, smaller footprint and fewer environmental concerns. In Japan com-

\* Corresponding author.

munication networks are demanding reduced costs and longer life from their batteries. Today, protection of the global environment is one of the most important issues facing the world. Research on, and the development of, power storage batteries for practical use are becoming more active with a view to power saving and a stable power supply. For this kind of application, more than 3000 cycles of battery life are required [5]. The deformation of positive electrodes due to corrosion is known to be the main factor in the life of a battery. We would therefore like to introduce our new material development of lead–calcium–tin (Pb–Ca–Sn) alloys and simulation technology of the deformation of positive electrodes due to corrosion as a predictive method to minimize the influence of corrosion.

## 2. Experimental

### 2.1. Preparation of alloy

The Pb–Ca–Sn alloys selected for study by the Taguchi method are listed in Table 1. These alloys are made by lead (99.99%) and tin (99.999%). The Pb–Ca–Sn ternary alloys were prepared by dissolving them in a fusion furnace covered with argon-gas at 773 K. Alloys were cast in a mould preheated to 473 K, then cooling the small test strips in jars filled with 273 K water just after solidification; the small test strips were 110 mm × 29 mm × 2 mm in size. The sample cast for microscopy was a 2 mm × 3 mm × 80 mm test piece, which was cut off using a precision saw and 50 mm was used. The test piece was analyzed by inductively coupled plasma analysis.

### 2.2. Metallurgical microscope observation

The measured object plane was a cross section, which was longitudinally vertical in the center of the sample. It was adjusted to a time of about 5 h from the casting to the end of polishing order to harden polishing and minimize the heat treatment. A metallurgical microscope was used to observe the metal structure of the test piece.

Table 1  
Chemical analysis using inductively coupling plasma spectrometer of Pb–Ca–Sn alloys

No.	Nominal composition (wt.%)		Analytical composition (wt.%)	
	Ca	Sn	Ca	Sn
1	0.1	1.0	0.087	0.92
2	0.1	1.6	0.087	1.45
3	0.1	2.0	0.095	2.09
4	0.08	1.0	0.075	1.08
5	0.08	1.6	0.073	1.68
6	0.08	2.0	0.071	2.01
7	0.06	1.0	0.059	1.02
8	0.06	1.6	0.054	1.64
9	0.06	2.0	0.056	2.12

Table 2  
Age hardening condition

Factor	Test condition
Aging temperature (K)	293, 320, 353
Aging time (h)	0, 5, 10, 20, 50, 100, 200

### 2.3. Age hardening condition

Heat treatment was carried out under the conditions shown in Table 2 to examine the effect of alloy composition on age hardening. The sample was measured after cast or heat treatment within 30 min.

### 2.4. Micro hardness measurement

Micro-Vickers hardness was measured (under a loading charge of 98 N for 5 s) for each sample using a micro-Vickers hardness tester. Hardness data were determined from the average of at least six hardness readings from each sample.

### 2.5. Tensile strength tests

A tensile strength test machine was used for the tensile strength tests.

### 2.6. Battery tests

Positive plates using No. 5 and No. 8 alloy were mounted in cells. The battery test was made in a 344-K water bath.

## 3. Results and discussion

### 3.1. Metal structure

The structure of Pb–Ca–Sn alloys is shown in Fig. 1. The grain boundary is complicated, when the calcium content is greater than the amount of tin. The grain boundary becomes linear when the amount of tin is dominant, or if it is equal to the calcium content. The macrostructure can be classified into two characteristic groups by the calcium content; one group is 0.06% and the other over 0.08%. The grain size shows a bulky structure over 1 mm in the former. Moreover, the grain boundary is a straight line or a gentle curve in the former, while in the latter it is a minute structure and the grain boundary is irregular. According to Tsubakino [6], the precipitation of Pb–Ca–Sn alloy is not only dependent on calcium content; there is also an effect of the tin/calcium ratio, and an effect from  $Pb_3Ca$  discontinuous precipitation. When it changes to continuous precipitation of  $Pb_{3-x}Sn_xCa$ , the Pb–Ca–Sn alloy, as a material for use in lead storage batteries, can also be classified as shown in the phase diagram [7] Fig. 2. This alloy can be classified as shown in Table 3.

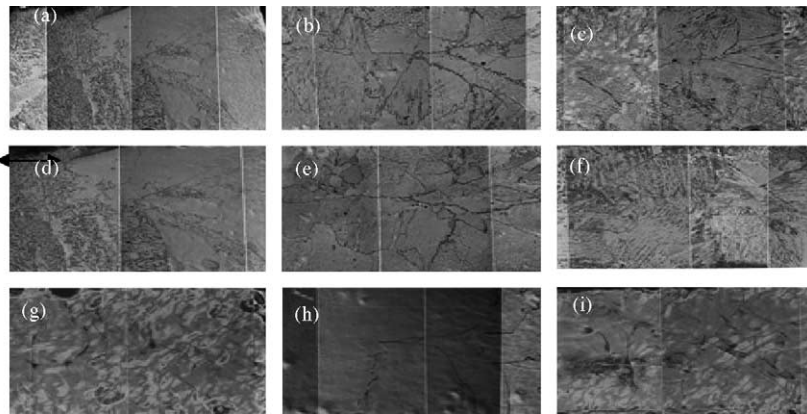


Fig. 1. Structure of Pb–Ca–Sn Alloy 0.5 mm field of view. (a) No. 1, (b) No. 2, (c) No. 3, (d) No. 4, (e) No. 5, (f) No. 6, (g) No. 7, (h) No. 8, (i) No. 9.

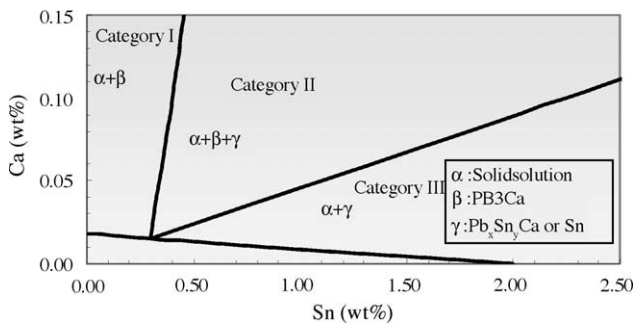


Fig. 2. Phase diagram of Pb–Ca–Sn alloy on lead–acid battery at casting process.

3.2. Battery life test

Life testing of the relationship between corrosion and deformation in a positive plate was examined to determine the effect of metal structure and mechanical property of the Pb–Ca–Sn alloy on the battery characteristic. Life transition of the discharge characteristics in the 344 K overcharge test is shown in Fig. 3. The definition of positive plate deformation volume is determined by the sum of the displacement derived from the overcharge test. The grid body underwent an elongation of especially the thick grid bars and the thin grid bars, because it was the combination of the grid bars in which the cross section differed.

Fig. 4 shows the relationship between grid cross section and grid strain rate. It shows that the deformation of the grid bars in which the cross section is thin greatly affects the deformation of the positive plate. Fig. 6 shows the relationship

Table 3  
Features and classification of the Pb–Ca–Sn alloy

Category	Alloy no.	Composition	Structure	Grain boundary
I	1, 4	$\alpha + \beta$	Minute structure	Irregular for the saw.
II	2, 3, 5, 6	$\alpha + \beta + \gamma$	Large structure	Slightly irregular for the saw
III	7, 8, 9	$\alpha + \gamma$	Large structure	Describes straight line or gentle curve

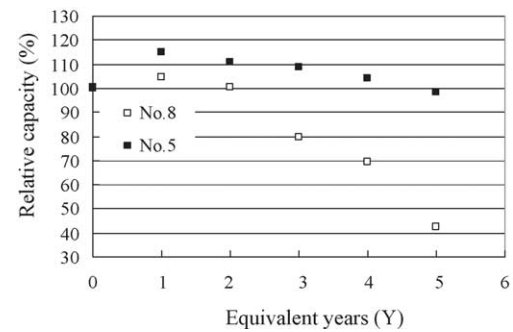


Fig. 3. Comparison of No. 5 and No. 8 alloy on discharge capacity during overcharge test.

between grid cross section and grid strain rate. Fig. 5 shows the relationship between corrosion quantity and positive electrode deformation.

Though the deformation volume increases in the No. 5 alloy with the corrosion, the relation is not as clear in the No. 8 alloy. Thus, the material could be approved for a battery design, because alloy of category II including the No. 5 alloy estimates that the quantity of corrosion for the permitted life that is possible, was proven. The battery was disassembled to learn the difference in the deformation condition depending on the material, and the amount of corrosion of the positive electrode grid and deformation volumes of the positive plate were examined.

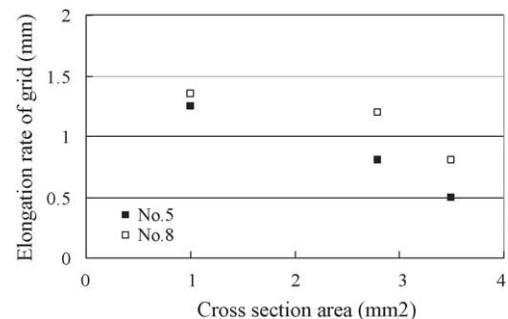


Fig. 4. Relationship between grid cross section and grid strain rate.

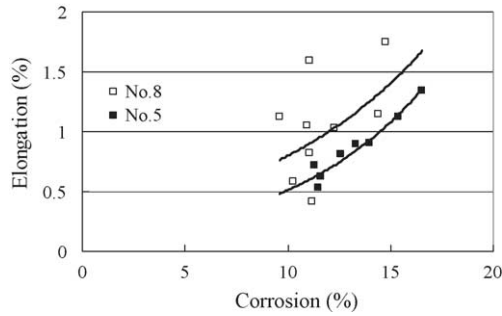


Fig. 5. Relationship between corrosion quantity and positive electrode deformation.

Cross section photographs are shown in Fig. 6. Though the No. 5 alloy shows general uniform corrosion, No. 8 alloy seemed to be the cause of the difference of the deformation, because there was intergranular corrosion, which had deeply invaded the No. 8 alloy [8,9]. This result clarifies the characteristics of the Pb–Ca–Sn alloy, because there seems to be an analogy between the metal structure and mechanical property, which is important.

Fig. 5 shows that the deformation is exponentially extended by the grid corrosion.

The cubical expansion is generated by the corrosion because the specific volume of lead sulfate and lead dioxide of the corrosion product is greater than that of the lead. In VRLA the stress by the cubical expansion acts to elongate the grid, because the plates are pressed.

In short, the cause of the elongation is the cubical expansion of the grid, and it seems to be because the elongation arises as the ratio increases.

In the case of trickle charge application, it is believed to depend on the period of use, if conditions of the corrosion layer thickness of the grid are equal (temperature, voltage, battery structure and specification). The result shows that it takes on an unequal shape, as the thin grid bar with relatively small cross section grows when the cross section of grid is different.

### 3.3. Simulation of the positive electrode deformation using computer aided engineering (CAE)

If, though deformation and displacement are generated, it is assumed that the elongation of the grid corrosion arises uniformly, the form does not change. However, there are many cases in which the corrosion has actually been unequal. Here, VRLA is considered.

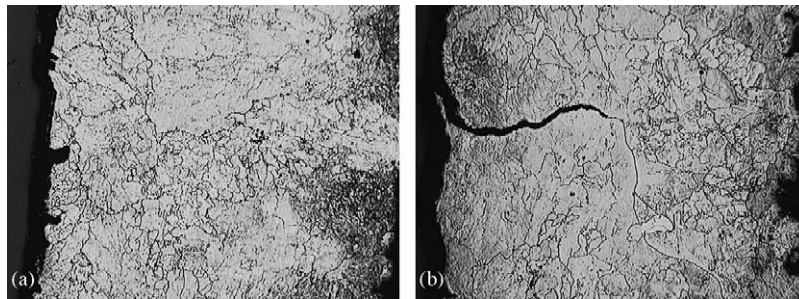


Fig. 6. Cross section of positive electrode after over charge test. (a) No. 5 alloy (b) No. 8 alloy.

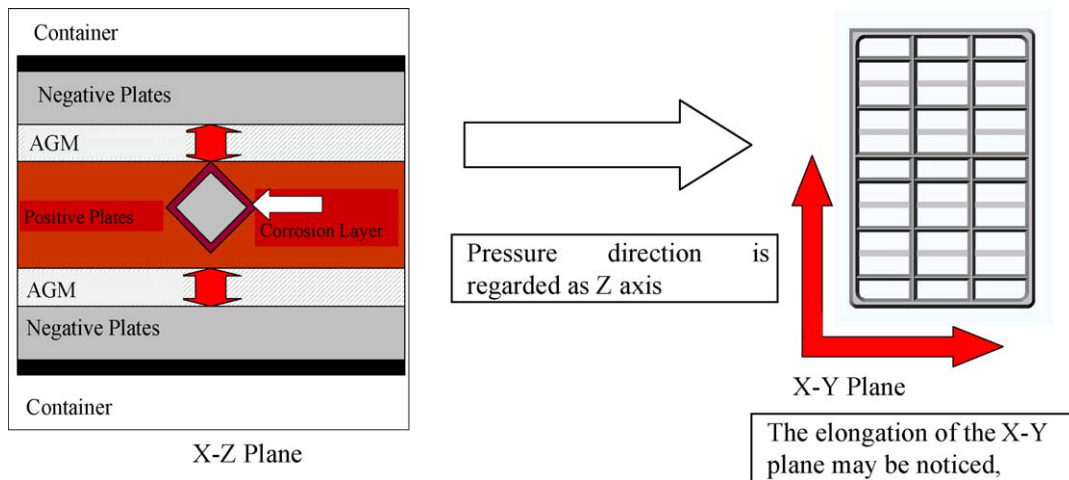


Fig. 7. Mechanism of the grid corrosion deformation.

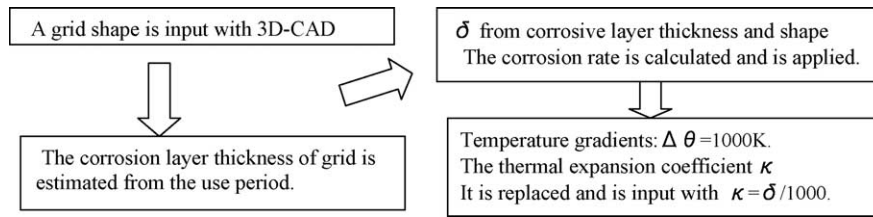


Fig. 8. Method of grid corrosion deformation simulation.

Fig. 7 shows the mechanism of the grid corrosion deformation. The elongation of the X–Y plane can be noticed when the pressure direction is regarded as the Z-axis, because the oppression force is applied in the lamination direction of the assembled element. This element receives the compressive force in the lamination direction. The grid body is filled with the active material when the plates of the lead storage battery are considered. Based on these two factors, it is possible that the normal direction of grid cross section extends when there is cubical expansion and when metallic lead which is the grid body of the positive plates corrodes. In short, it is possible that the problem of the metallic lead being cubically expanded by the corrosion is replaced by the linear expansion problem in the X–Y plane. The finite element method is considered by the fixing the Z-axis as the initiator of the elongation problem in the X–Y plane. Using the shape of the grid body with a corrosion rate (deformation degree) that is different and generates the unequal deformation, the corrosion rate of every shape classified by cross section was calculated when the cross section which had formed the grid body was different, even if the corrosion (thickness) of the grid had advanced uniformly, since the progression of the corrosion was different. Fig. 8 shows a flow chart of the simulation method.

Table 4

Replacement of thermal expansion problem and corrosion deformation problem

	Thermal deformation problem	Corrosion deformation problem
Intensive variable	Thermal expansion coefficient	Parameter on the corrosion deformation
Extensive variable	Temperature gradient	Use period (frequency)

Table 4 shows a replacement of the thermal expansion problem and the corrosion deformation problem.

3.4. An example of applying the grid deformation simulation analysis using ANSYS (general-purpose CAE software)

Fig. 9 shows corrosion behavior and simulation results of the grid body following 3-year use of VRLA of the 7 Ah–12 V type. It is seen that the simulation agrees well, if the conditions fit the figure well.

In short, the approach described so far is correct. Weight of the active materials was increased by 10% in simulation and change and elongation of the shape were noticed. Table 5 shows the design condition and analytical results of the design. Fig. 10 shows the bare grid shape and its simulation

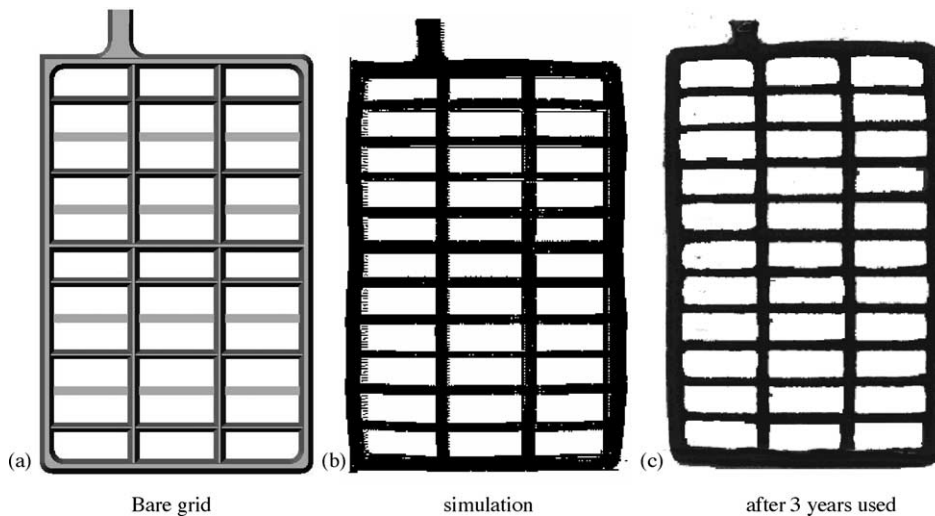


Fig. 9. Corrosion behavior and simulation result of grid after the 3-year use of VRLA of the 7 Ah–12 V type.

Table 5  
Design condition and analytical result of the design

No.	Design	Vertical elongation (%)	Horizontal elongation (%)
a	Base	100	100
b	Inner grid bars 50% shaped	200	127
c	Flame grid bars 60% shaped	246	118
d	Similar unit with uniform cross section	254	65
e	Design (similar unit)	160	68

result. The deformation volume also increased beyond the standard in either case, which is further proof that changes of the structure were necessary to utilize the original design.

Especially, it was proven that the deformation volume increased when the cross section of the thick grid element,

which supports the plate was lowered. This was the same in all cross sections, using shape, which divided the whole into similar lattice unit. This shape is known as a design in which the power collection of the grid is advantageous if it is the identical weight.

However, the shape was examined in this design, because the deformation volume compared with the standard design was proven. That it is not similar is due to fluidity and gradient of the mould release.

The whole elongation is increased because there is no grid with a cross section thick enough to support the whole when this shape is used. To some extent, unequal deformation could retain the deformation by distributing the grid element inside the frame, in order to decrease the overall deformation. It was proven that equal deformation transformed

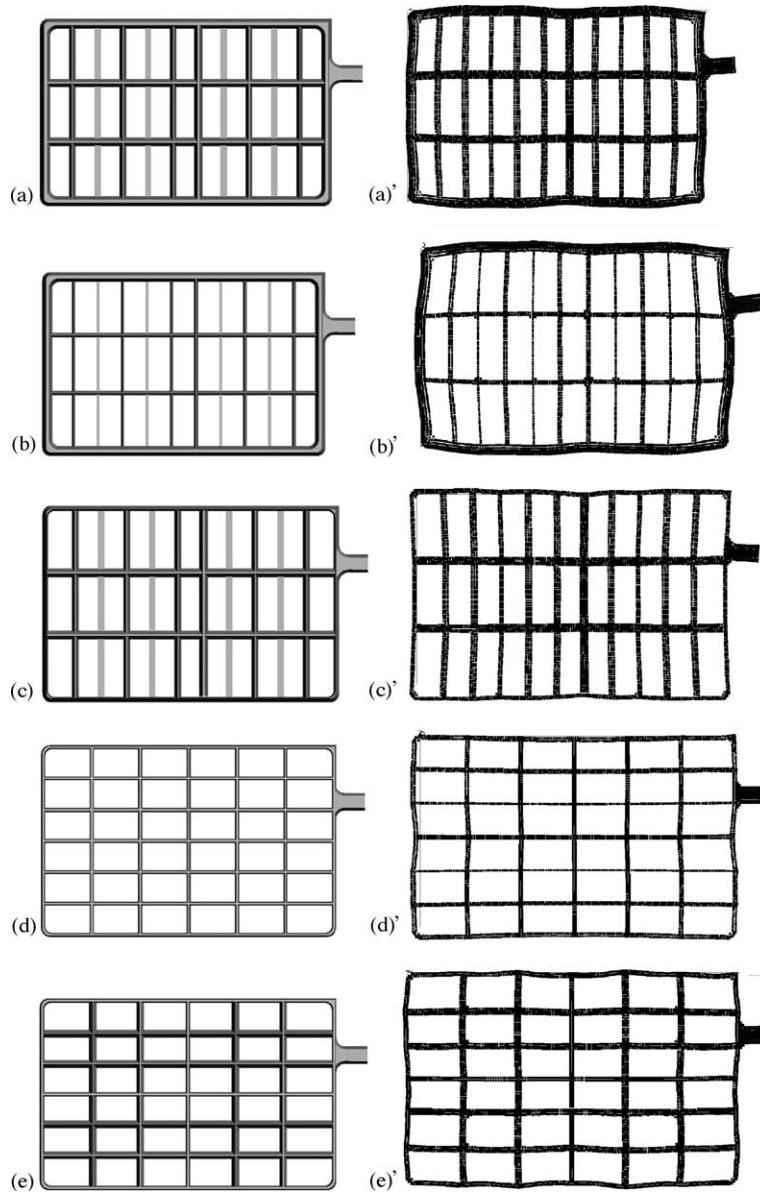


Fig. 10. Bare grid shape (a)–(e) and simulation result of grid (a)'–(d)'.

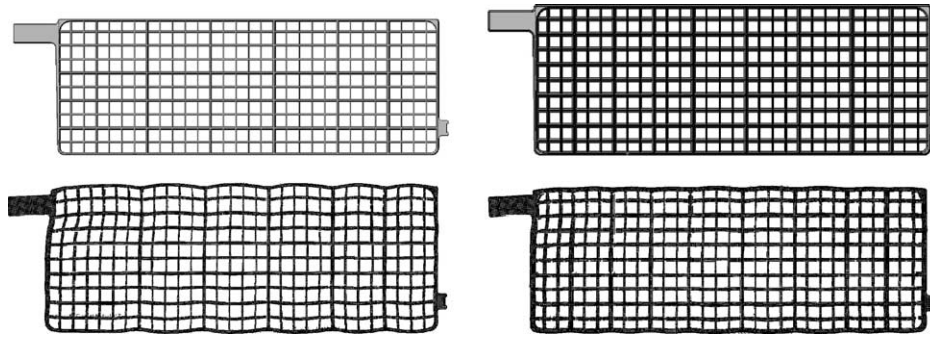


Fig. 11. Bare grid shape (top) and its analytical result (bottom) of the conventional (left) and development (right).

the deformation similarly and made the whole elongation small.

### 3.5. Simulation of the positive electrode deformation using the CAE for battery development

By optimizing the alloy composition, a simulation was carried out to estimate the deformation condition, and lifetime corrosion was predicted. The result calculated using general-purpose simulation software ANSYS (Cybernet Systems Co., Ltd.) and replacing the corrosion deformation with thermal deformation is shown in Fig. 11. It shows bare grid shape and its analytical result of the development compared with a conventional grid. The analytical result is independent software, because the result was similar even in ADSTFAN (Hitachi, Ltd.) using ANSYS.

It was possible that in this case the design also lengthens the cycle life further and decreases the deformation volume further than the conventional design.

### 3.6. Development of the new simulation technique

In the conventional method [10], it is necessary to separate the material from the ratio of corrosion thickness and thickness of the grid bar. Though it does not become a problem in thick 2 types, it becomes very troublesome work as the thickness of the grid bar delicately differs, or is defined as a different material in the data preparation. The method for

replacing the corrosion phenomenon with the temperature diffusion was applied, because the corrosion phenomenon is also a kind of diffusion phenomenon.

In short, the method used sulfuric acid in which the oxidation of the grid electrochemically replaced the corrosion layer formation to diffuse the temperature. Heat is given, from the surface of the grid, and this method replaced the problem in which the grid is expanded by the high-temperature on the surface. This could be calculated without setting the thermal expansion coefficient, which depends on the cross section used in the conventional approach. However, the solution of the casting analysis software; Adstefan of finite element difference calculus was added, because it is not possible, that this method was applied in general-purpose software. ANSYS is made to form the thermal diffusion part which corresponds to the corrosive layer, and it is replaced with the thermal expansion problem. Here, it is called Adstefan-plus.

(1) The procedure of the technique analysis which quantitatively puts temperature distribution and the corrosion progress situation together is shown in the following.

Fig. 12 is a model figure of the mesh division. It is made to be a  $882 \times 282 \times 14$  (total: 3482136 mesh) model as 0.5 mm mesh size.

(2) An unsteady thermal analysis was carried out, and the temperature distribution result which the progress of temperature diffusion and corrosion becomes equivalent is deduced.

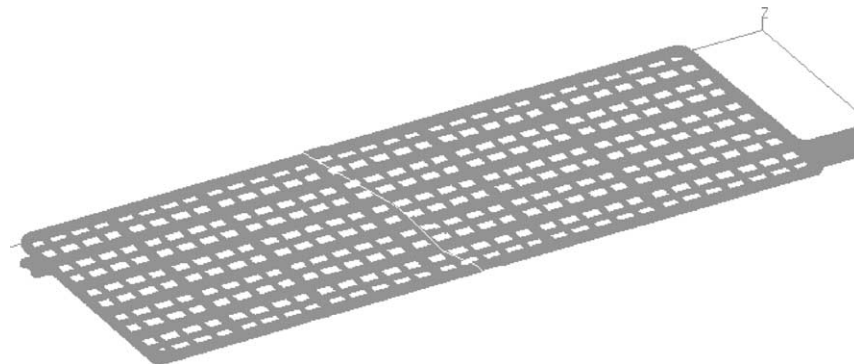


Fig. 12. Model figure of the mesh division.

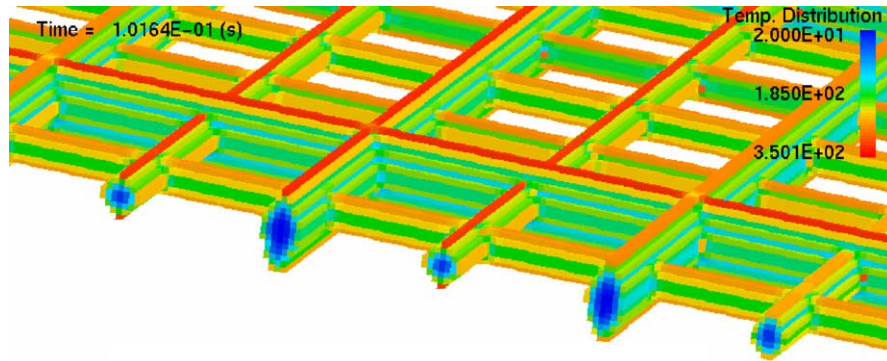


Fig. 13. Corrosion layer formation model by the temperature.

Fig. 13 shows the corrosion layer formation model according to the temperature.

By setting the analysis hour at an extreme time with 0.1 s, it is possible to deduce the temperature distribution in order to realize the temperature change on only the surface of the grid.

- (3) The temperature rise per minute is converted into the elongation, and thermal stress analysis was carried out. The deformation analysis under the same condition was carried out on the design shown in the analytical result table on the lead grid shape model. Though the result has been omitted, it would be possible to estimate the corrosion deformation volume in the examination stage of the grid, if grid corrosion deformation simulation were used.

#### 4. Conclusion

By determination of the properties of Pb–Ca–Sn alloy and considering the application of the lead storage battery, it is possible to choose the optimal material for this battery. By combining the CAE with features of this material, lifetime prediction of the battery may be made more reliable.

The design of the lead storage battery grid decides grid weight, and space volume (the active material retention),

plate thickness are decided from the battery characteristic. Therefore, it is effective as an instrument of Potential Problem Analysis and allows consideration to be given to other problems which may affect safety factors, rather than limit in the design analysis to a consideration of corrosion deformation.

#### References

- [1] R. David Prenagaman, *The Battery Man*, vol. 39, September 1997, p. 16.
- [2] I. Mukaitani, T. Sakamoto, T. Kikuoka, H. Tsubakino, *Proceedings of the 40th Battery Symposium in Japan*, 1999, p. 99.
- [3] I. Mukaitani, K. Hayashi, I. Shimoura, H. Takabayashi, M. Terada, A. Takemasa, I. Takahashi, K. Okamoto, *Proceedings of the 40th Battery Symposium in Japan*, 2003, p. 652.
- [4] A. Takemasa, I. Mukaitani, Y. Yoshiyama, K. Fukui, T. Sakamoto, T. Kuwano, M. Fukuda, H. Misaki, K. Uwatari, *Shin-Kobe Tech. Rep.* 9 (1999) 11.
- [5] H. Takabayashi, T. Shibahara, Y. Mastuda, K. Fukui, S. Hazui, Y. Matsumura, S. Kondo, *Shin-Kobe Tech. Rep.* 11 (2001) 35.
- [6] H. Tsubakino, M. Tagami, S. Ioku, A. Yamoto, *Metall. Mater. Trans. A* 27A (1996) 1675.
- [7] P. Adeave, et al., *Mater. Sci. Eng.* 54 (1982) 229.
- [8] H. Giess, *J. Power Sources* 53 (1995) 31.
- [9] D. Kelly, P. Niessen, E.M.L. Valeriotte, *J. Electrochem. Soc.* 132 (1985) 2533.